Fat-Constrained Reconstruction of 18F FDG Accumulation in an Integrated PET/MR System using MR Dixon Imaging

Sven Prevrhal[1], Susanne Heinzer[2], Bénédicte Delattre[2,3], Steffen Renisch[4], Christian Wülker[5], Osman Ratib[3], and Peter Börnert[1]

[1]Philips Research, Hamburg, Germany, [2]Philips AG Healthcare, Zurich, Switzerland, [3]University Hospital of Geneva, Geneva, Switzerland, [4]Philips Research, Hamburg, Deutschland, Germany, [5]University of Heidelberg, Germany

Introduction: The fusion of the information from PET and MRI can increase the diagnostic value of both modalities. PET is clinically very useful to image metabolic processes and physiologic function, whereas MRI shows excellent soft tissue contrast. This complementarity has spawned first generations of multi-modality PET/MR devices. In such systems, MR imaging can be exploited for motion correction of PET data (1) or to estimate tissue attenuation of the PET signal for appropriate correction, improving the quality of quantitative results PET can deliver (2). However, in general, PET has limited spatial resolution compared to MRI. The overarching idea of this work is to improve the spatial resolution of the PET images by using anatomical MR images as prior information for the PET image reconstruction process beyond standard attenuation correction. We used the working hypothesis that fatty tissue metabolism is low in glucose consumption. Thus, a PET tracer like ^{18}F-deoxyglucose (FDG) should have limited accumulation in fatty tissue and generate insignificant PET signal in this compartment. The spatial fat distribution can be extracted from water/fat-resolved mDixon MR images forming an input, a negative anatomical MR prior, for an appropriately modified PET reconstruction to improve accuracy of PET images in such regions.

Methods: In this work, water/fat-resolved 3D whole body scanning was used on a commercial time-of-flight PET/MRI system (Ingenuity TF with Achieva 3T MRI, Philips Healthcare). Phantom and *in vivo* experiments were performed. Patients were included with informed consent obtained. The basic MRI sequence parameters for each of the mult i-station 3D volumes were: two-point mDixon gradient echo (α:7°,TR/TE1/TE2: 3.3/1.1/2.1ms, voxel size: 1.6×1.6×4 mm³, FOV(RL,AP,FH): 500×390×120 mm³ yielding water and fat images after separation (3). Phantom PET/MR scans were performed using the standard NEMA/IEC Body Phantom, which contains structures visible on PET and MR images. Following IEC recommendations for test conditions, the body cylinder was filled with water with an ^{18}F-FDG activity concentration of 5.3 kBq/ml (typically seen background in patient FDG studies), but only in its bottom half. The top half was filled with nonradioactive standard corn oil to test the new constraint algorithm. The two largest sphere inserts of the phantom were filled with nonradioactive water, whereas the other spheres were filled with ^{18}F-FDG with activity concentration equal to four times the background signal, again according to IEC recommendations. *In vivo* PET/MR measurements were performed in two tumor patients (15 and 43 years). List-mode time-of-flight OSEM PET reconstruction (4) was performed natively and with the fat prior constraint. The constraint was implemented via a modification to the on-the-fly system matrix calculation (4), similar to the way time-of-flight weighting is incorporated: An additional voxel weight reflecting fat content was added to the forward- and back-projection signal operations for each line of coincidence (LOC). As a consequence, PET signal activity is shifted along the LOC into regions which do not show much fat content. This additional constraint was scaled by a parameter c [-0.3, 0.3] to heuristically limit the influence of fat weighting.

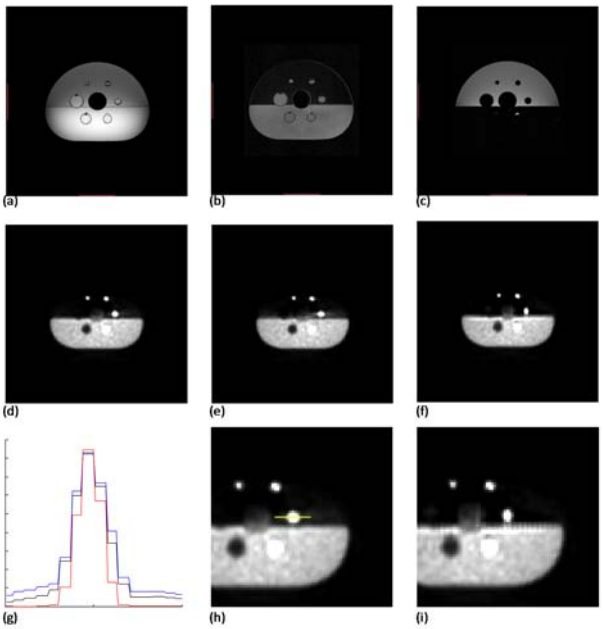

Fig. 1. IEC phantom filled with water in the bottom and oil in the top. (a) native gradient echo MRI, (b) mDixon water, (c) mDixon fat, (d) native PET image, (e) fat-control PET (weight +0.1), (f) fat-constrained PET (weight -0.3), (g) Signal profiles (yellow line shown in (h)) black: native PET, blue: reverse control PET, red: fat-constrained PET with close ups in (h=d, i=f).

Results and Discussion: Figure 1 shows gradient-echo mDixon (a-c) and the native and fat-constrained PET reconstructions (d-f). Using the fat-constrained PET reconstruction, resolution enhancement is clearly visible for the correctly weighted prior strength (f) and reversed in a control reconstruction (e). The gray value profiles in (g) show the reduced partial volume effects quantitatively and better SNR for various weights vs. native PET reconstruction. Note that the apparent activity in the center lung tissue-mimicking insert is a spurious result of the attenuation correction algorithm which is optimized for humans. The same holds for the *in vivo* data shown in Fig.2. Increased uptake in the left breast is clearly visible comparing the native versus the fat-weighted reconstructions. Also conforming to expectation, the fat-constrained down-weighted reconstruction showed reduced uptake in areas with high fat content (yellow arrow) and increased uptake in low-fat areas (green, red arrows). The control fat-constrained up-weighted images showed inverse behavior. In the other patient (15 years old), strong PET signal was found in the neck/shoulder region, which is known to be a preferred location for brown fat (5) and hypermetabolic (high vascularity and mitochondrial density) showing PET signal uptake. Uptake appears lowered in the Dixon-constrained reconstruction, consistent with the design of the algorithm. The information about the potential location of brown fat could be integrated into future constrained modeling.

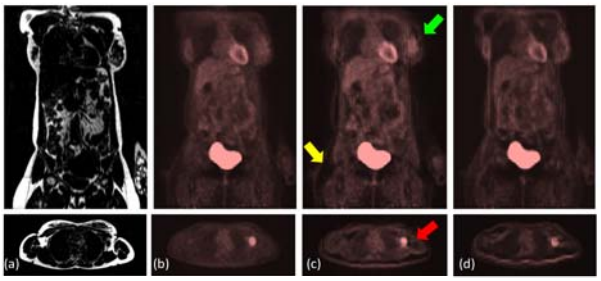

Fig.2. Patient - coronal/axial MR and PET data. (a) mDixon fat coronal mid- and fat axial breast-slice, adapted to PET resolution, (b) native PET/MR list-mode time-of-flight OSEM reconstruction. (c) fat down-weighted PET, (d) control fat up-weighted PET image. Fat-constraining effects are clearly demonstrated in uptake in the breast (green arrow) and lymph nodes (red arrow). In the fat-down-weighted images PET signal from subcutaneous depots (yellow arrow) is reduced.

Conclusion: The use of the fat compartment information delivered by Dixon MR in a hybrid PET/MR system to constrain time-of-flight list-mode reconstruction of PET/MR resulted in reduced PET image intensity in areas of fatty tissue and image enhancement of adjacent high-uptake regions and may contribute to increased spatial resolution and thus the potential diagnostic value of PET. The technique explored in this early report on the use of MR information to guide PET reconstruction may prove generally useful in PET/MR imaging and can benefit further from other contrasts deliverable by MR.

References: [1] Tsoumpas C. et al. Ann Nucl Med. 2010;24:745-50. [2] Schulz V. et al. Eur J Nucl Med Mol Imag. 2011;38:138-52. [3] Eggers H. et al. MRM 2011; 65:96-107. [4] Hu, Z. et al. IEEE Nucl. Science. Symp. 2006 6, 3392–3396 (2006). [5] Hu HH. et al. AJR Am J Roentg. 2013; 200:177-83.